

Published in final edited form as:

Toxicol Appl Pharmacol. 2014 October 1; 280(1): 127–137. doi:10.1016/j.taap.2014.06.028.

Cyanidin-3-Glucoside inhibits UVB-induced oxidative damage and inflammation by regulating MAP kinase and NF- κ B signalling pathways in SKH-1 hairless mice skin

Poyil Pratheeshkumar^{a,b}, Young-Ok Son^{a,b}, Xin Wang^{a,b}, Sasidharan Padmaja Divya^{a,b}, Binoy Joseph^c, John Andrew Hitron^{a,b}, Lei Wang^{a,b}, Donghern Kim^b, Yuanqin Yin^{b,d}, Ram Vinod Roy^{a,b}, Jian Lu^{b,e}, Zhuo Zhang^b, Yitao Wang^f, and Xianglin Shi^{a,b,*}

^a Center for Research on Environmental Disease, University of Kentucky, 1095 VA Drive, Lexington, KY 40536, USA.

^b Graduate Center for Toxicology, University of Kentucky, 1095 VA Drive, Lexington, KY 40536, USA.

^c Spinal Cord and Brain Injury Research Center and Department of Physiology, University of Kentucky, Lexington, KY 40536-0509, USA.

^d Cancer Institute, The First Affiliated Hospital, China Medical University, Shenyang, China.

^e Institute of Life Sciences, Jiangsu University, Zhenjiang, Jiangsu, China, 212013

^f State Key Laboratory of Quality Research in Chinese Medicine, Institute of Chinese Medical Sciences, University of Macau, Macau, China

Abstract

Skin cancer is one of the most commonly diagnosed cancers in the United States. Exposure to ultraviolet-B (UVB) radiation induces inflammation and photocarcinogenesis in mammalian skin. Cyanidin-3-Glucoside (C3G), a member of the anthocyanin family, is present in various vegetables and fruits especially in edible berries, and displays potent antioxidant and anticarcinogenic properties. In this study, we have assessed the *in vivo* effects of C3G on UVB irradiation induced chronic inflammatory responses in SKH-1 hairless mice, a well-established model for UVB-induced skin carcinogenesis. Here, we show that C3G inhibited UVB-induced skin damage and inflammation in SKH-1 hairless mice. Our results indicate that C3G inhibited glutathione depletion, lipid peroxidation and myeloperoxidation in mouse skin by chronic UVB exposure. C3G significantly decreased the production of UVB-induced pro-inflammatory

© 2014 Elsevier Inc. All rights reserved.

*Corresponding author Xianglin Shi, Ph.D., Professor William A. Marquard Chair in Cancer Research Graduate Center for Toxicology Director, Center for Research on Environmental Disease Associate Director for Cancer Chemoprevention and Environmental Toxicology Markey Cancer Center University of Kentucky 232 Bosomworth #HSRB Lexington, Kentucky 40536-0001 (859) 257-4054 (office) (859) 323-1059 (fax) xshi5@email.uky.edu.

Publisher's Disclaimer: This is a PDF file of an unedited manuscript that has been accepted for publication. As a service to our customers we are providing this early version of the manuscript. The manuscript will undergo copyediting, typesetting, and review of the resulting proof before it is published in its final citable form. Please note that during the production process errors may be discovered which could affect the content, and all legal disclaimers that apply to the journal pertain.

Disclosure of Potential Conflicts of Interest: No potential conflicts of interest were disclosed.

cytokines, such as IL-6 and TNF- α , associated with cutaneous inflammation. Likewise, UVB-induced inflammatory responses were diminished by C3G as observed by a remarkable reduction in the levels of phosphorylated MAP Kinases, Erk1/2, p38, JNK1/2 and MKK4. Furthermore, C3G also decreased UVB-induced cyclooxygenase-2 (COX-2), PGE₂ and iNOS levels, which are well-known key mediators of inflammation and cancer. Treatment with C3G inhibited UVB-induced nuclear translocation of NF- κ B and degradation of I κ B α in mice skin. Immunofluorescence assay revealed that topical application of C3G inhibited the expression of 8-hydroxy-2'-deoxyguanosine, proliferating cell nuclear antigen, and cyclin D1 in chronic UVB exposed mouse skin. Collectively, these data indicates that C3G can provide substantial protection against the adverse effects of UVB radiation by modulating UVB-induced MAP kinase and NF- κ B signaling pathways.

Keywords

Cyanidin-3-Glucoside; Ultraviolet radiation; inflammation; COX-2; NF- κ B

Introduction

Ultraviolet (UV) light has been recognized as a complete carcinogen, responsible for both initiation and promotion of skin carcinogenesis, and disrupting immune homeostasis (Ananthaswamy and Pierceall, 1990). The immediate harm and long-term health risks of excessive sunlight exposure are impairing the lives of people worldwide. Inflammation is a key mechanism underlying UVB's various detrimental effects (Sano and Park, 2014). Reactive oxygen species (ROS) plays a major role in the development of UVB induced skin cancer. There is considerable evidence that UVB-induced ROS mediates the phosphorylation of protein kinases through a series of cascades, such as mitogen-activated protein kinases (MAPK), a well-known contributing factor to skin carcinogenesis (Sharma *et al.*, 2007).

Chronic UVB exposure induces constitutive expression of cyclooxygenase-2 (COX-2), which is the primary source of elevated prostaglandin E₂ (PGE₂) in the skin. This increases prostaglandin synthesis which plays a key role in carcinogenesis by contributing to uncontrolled proliferation of damaged cells that ultimately form tumors (Burns *et al.*, 2013). Nuclear factor κ B (NF- κ B) is another major factor mediating UVB-induced inflammatory responses through the expression of various proinflammatory proteins such as inducible nitric oxide synthase (iNOS), Tumor necrosis factor- α (TNF- α) and Interleukin-6 (IL-6) (Sharma and Katiyar, 2010; Choi *et al.*, 2014). UVB also indirectly damages DNA by increasing levels of ROS which facilitate oxidative damage to DNA bases, inducing the formation of 8-oxo-7, 8-dihydro-2'-deoxyguanosine (8OHdG) (de Gruijl, 2002). In addition, UVB-induced DNA damage in the form of cyclobutane pyrimidine dimers (CPDs) has also been implicated in skin cancer risk (Vaid *et al.*, 2010).

The use of dietary botanicals with substantial antioxidant and anti-inflammatory activities to protect the skin from the adverse biological effects of solar radiation is receiving increasing attention. Cyanidin-3-glucoside (C3G) is a naturally occurring polyphenolic anthocyanin

widely distributed in fruits, vegetables, and pigmented cereals (Zheng and Wang, 2003). C3G is a potent antioxidant and displays anti-cancer properties *in vitro* and *in vivo* (Chen *et al.*, 2005; Shih *et al.*, 2005; Ding *et al.*, 2006; Xu *et al.*, 2010). In our previous studies C3G inhibited skin tumor promotion in 7,12- dimethylbenz(a)anthracene (DMBA)-initiated and 12-*O*-tetradecanoyl phorbol-13-acetate (TPA)-promoted skin carcinogenesis model. C3G also inhibited UVB- and TPA-induced transactivation of NF- κ B, AP-1, COX-2 and TNF- α in JB6 cells (Ding *et al.*, 2006).

In this study, we investigated the protective effect of C3G on UVB-induced inflammation and early biomarkers associated with photocarcinogenesis in SKH-1 hairless mouse skin model. We found that topical application of C3G to SKH-1 hairless mice prior to UVB radiation resulted in a significant inhibition of UVB-induced (i) skin edema, hyperplasia, and infiltration of leukocytes; (ii) COX-2, iNOS and PGE₂ production; (iii) elevated proinflammatory cytokines level (TNF- α and IL-6); (iv) increase in the cell proliferation protein markers (PCNA and cyclin D1); (v) phosphorylation of ERK1/2, JNK1/2, p38 and MKK4 protein expressions; (vi) Oxidative stress and formation of 8-OHdG & CPDs; and (vii) activation of NF- κ B and IKK α , and degradation of I κ B α .

Materials and methods

Animals

The female SKH-1 hairless mice (6–7 weeks old) were purchased from Charles River Laboratory (Wilmington, MA). The mice were acclimatized for at least 1 week before experimental use in the animal resource facility and maintained under standard conditions of a 12 h dark/12 h light cycle at a temperature of $24 \pm 2^\circ$ C and relative humidity of $50 \pm 10\%$. The animal protocol used in this study was approved by the Institutional Animal Care and Use Committee of the University of Kentucky at Lexington.

Antibodies and chemicals

Antibodies specific for p-P38, P38, p-MKK4, MKK4, and iNOS were obtained from cell signaling Technology (Beverly, MA). The primary antibodies specific for proliferating cell nuclear antigen (PCNA), p-ERK, ERK, p-JNK, JNK, NF- κ B/p65, IKK α , I κ B α , COX-2, TNF- α , cyclin D1, β -actin and the secondary antibodies were purchased from Santa Cruz Biotechnology, Inc. (Santa Cruz, CA). Assay kits for Myeloperoxidase Peroxidation (MPO), Glutathione (GSH) and an immunoassay kit for prostaglandin E₂ (PGE₂) analysis were obtained from Cayman Chemical (Ann Arbor, MI). Assay kit for thiobarbituric acid reactive substances (TBARS) was purchased from BioAssay Systems (Hayward, CA, USA). Enzyme-linked immunosorbent assay kits specific for mouse tumor necrosis factor (TNF)- α and interleukin-6 (IL-6) were obtained from PromoKine (Heidelberg, Germany). Cyanidin 3-glucoside (C3G) was purchased from Polyphenols Laboratories AS (Sandnes, Norway) and was dissolved in acetone for the topical application.

UVB light source and irradiation protocol

The SKH-1 hairless mice were exposed to UV irradiation with a distance of 23 cm between the light source and the target skin. The mice were randomly divided into 6 groups with 12

mice/group. The mouse dorsal skin was topically administrated with either acetone (control group, 50 l/mouse) or C3G (250 and 500 μ M in acetone) a day before UV exposure to avoid possible sunscreen effect. The mice were then exposed to 100 mJ/cm² of UVB for 3 times per week up to 10 weeks. Mice were exposed to UV radiation from a band of four FS24T1 UVB lamps (Daavlin, UVA/ UVB Research Irradiation Unit, Bryan, OH) equipped with an electronic controller to regulate UV dosage. At 2 h and 24 h of post UVB irradiation, the animals were euthanized and dorsal skin tissues were excised for designed experiments.

Immunoassay for quantitation of PGE₂

The analysis of PGE₂ in skin samples was performed using the Cayman PGE₂ Enzyme Immunoassay Kit (Ann Arbor, MI) following the manufacturer's protocol. Briefly, skin samples were homogenized in 100 mM phosphate buffer, pH 7.4 containing 1 mM ethylenediamine tetra acetic acid and 10 μ M indomethacin using a polytron homogenizer (Fisher Scientific, GA). The supernatants were collected and analyzed for PGE₂ concentration.

Tissue glutathione assay

Mouse skin tissue was homogenized in cold buffer (50 mM Phosphate, pH 6-7, containing 1 mM EDTA) and centrifuged at 10,000 g for 15 min at 4 °C. The supernatants were collected and the total GSH content was determined by Cayman's GSH assay kit (Cayman Chemical Co., Ann Arbor, MI) following the manufacturer's instruction.

TBARS assay

Lipid peroxidation was determined using a QuantChrom™ TBARS assay kit. Skin tissue was homogenized by sonication in ice cold PBS. After centrifugation at 12,000 g for 15 min at 4°C, the supernatant was assayed according to the manufacturer's instructions. Reacted samples were added to wells of a 96 well plate and were measured spectrophotometrically at 532 nm using MDA as a standard.

MPO assay

Tissue Myeloperoxidase was measured using Cayman's MPO Peroxidation assay kit (Cayman Chemical Co., Ann Arbor, MI) according to the manufacturer's instructions. In brief, this assay provides a fluorescence-based method for detecting the MPO peroxidase activity in tissue lysates. The assay utilizes the peroxidase component of MPO, and the reaction between H₂O₂ and 10-acetyl-3,7-dihydroxyphenoxazine (ADHP) produces the fluorescent compound resorufin.

Assay for proinflammatory cytokines

Epidermal homogenates from each treatment group were used for the analysis of cytokines, such as TNF- α , and IL-6, using enzyme linked immunosorbent assay kits (Promokine) following the manufacturer's instructions and reagents.

ELISA for NF- κ B/p65

For quantitative analysis of NF- κ B/p65, Trans™ ELISA kit (Active Motif, Carlsbad, CA) was used following the manufacturer's protocol. For this assay, the nuclear extracts of epidermal skin samples from various treatment groups were prepared using the Nuclear Extraction kit (Active Motif) according to the manufacturer's direction. Absorbance was recorded at 450 nm with reference taken at 650 nm. The assay was done in duplicate and the results are expressed as the percentage absorbance of control (non-UVB exposed) group.

Histopathological analysis

Skin samples from mice were fixed in 10% neutral buffered formalin and processed for paraffin-wax embedded sectioning of 4-6 m thick, stained with hemotoxylin and eosin dye and evaluated under light microscope.

Western blot analysis

Epidermis from the whole skin was separated and homogenized in ice-cold RIPA buffer (Sigma-Aldrich) with freshly added protease inhibitor cocktail. The homogenate was then centrifuged at 14 000 g for 25 min at 4°C and the supernatant (total cell lysate) were collected, aliquoted and stored at -80°C. Nuclear and cytoplasmic extracts were prepared using a nuclear and cytoplasmic extraction kit from Thermo Scientific (Rockford, IL) according to the manufacturer's protocol. The protein concentration was determined using Coomassie Protein Assay Reagent (Thermo, Rockford, IL). About 40 μ g cellular proteins were separated using 6%–12% SDS-polyacrylamide gel and transferred to nitrocellulose membrane. Membranes were blocked with 5% fat-free dry milk in 1X Tris-buffered saline (TBS) and incubated with antibodies. Protein bands were detected by incubating with horseradish peroxidase-conjugated antibodies (Pierce, Rockford, IL) and visualized with enhanced chemiluminescence reagent (Perkin Elmer, Boston, MA). To verify equal protein loading on the gel, the blots were stripped and reprobed for β -actin.

RNA extraction and quantitative Real-Time PCR

The total RNA was extracted from the mouse epidermis using TRIzol reagent (Invitrogen, CA) following the protocol recommended by the manufacturer. The mRNA expression of PCNA and cyclin D1 in skin samples was determined using real-time PCR, as detailed previously (Ding *et al.*, 2013). Reverse transcription of 3 μ g of total RNA was performed in a final volume of 20 μ l containing 5 X first strand buffer (Invitrogen), 1 mM of each dNTP, 20 units of placental RNase inhibitor, 5 μ M random hexamer, and 9 units of M-MLV reverse transcriptase (Invitrogen). After incubation at 37 °C for 45 min, 5 min at 92 °C to end the reaction, diluted at 1:4 and stored at -20 °C until PCR use. Using SYBR Green I (Molecular Probes, Eugene, OR), Two μ l of cDNA was subjected to real-time quantitative PCR with a BioRad MyiQ thermocycler and SYBR green detection system (BioRad, CA). Samples were run in triplicate to ensure amplification integrity. Manufacturer-supplied (SuperArray, Bioscience Corporation, MD) primer pairs were used to measure the mRNA expression of PCNA and cyclin D1. The standard PCR conditions were 95°C for 15 min, then 40 cycles at 95°C, 30 sec; 55°C, 30 sec; and 72°C, 30 sec, as recommended by the primer's manufacturer. The expression levels of genes were normalized to the expression

level of the β -actin mRNA in each sample. The threshold for positivity of real-time PCR was determined based on negative controls. For mRNA analysis, the calculations for determining the relative level of gene expression were made using the cycle threshold (Ct) method. The mean Ct values from duplicate measurements were used to calculate the expression of the target gene with normalization to a housekeeping gene used as internal control (β -actin), and using the 2^{-Ct} formula.

Immunofluorescence analysis

Skin samples were collected and frozen immediately in liquid nitrogen after embedding in optimal cutting temperature medium (OCT). The frozen skin samples were stored at -80°C for further use. Immunofluorescence staining was done to detect the NF- κ B/p65, 8-OH dG, TNF- α , PCNA and cyclin D1-positive cells. Briefly, frozen skin sections (5 μm thick) were fixed in ice cold acetone and nonspecific staining was blocked with 5% horse serum in PBS buffer. Specimens were probed with mouse anti-p65 (1:100; Santa Cruz, CA, USA), 8-OH dG (1:50; Santa Cruz, CA, USA), TNF- α (1:200; Novus Biologicals Inc, Littleton, CO), PCNA (1:100; Santa Cruz, CA, USA), cyclin D1 (1:50; Santa Cruz, CA, USA) antibodies and were subsequently incubated with secondary-Alexa Fluor 488-conjugated antibody (Molecular Probes, OR). Slides were then washed, and visualized using Zeiss Axio Observer inverted immunofluorescence microscope (Carl Zeiss MicroImaging GmbH, Gottingen, Germany).

Immunohistochemical detection of COX-2 and cyclobutane pyrimidine dimers

Five- μm thick frozen sections were hydrated in phosphate buffered saline (PBS), and then non-specific binding sites were blocked with 5% horse serum in PBS and preceded according to Vectastain ABC Kit protocol (Vector Laboratories, Burlingame, CA). Briefly, the sections were incubated with anti-COX-2 (1:100, Cell Signaling Technology, Beverly, MA) or anti-Cyclobutane pyrimidine dimer (1:100, Kamiya Biomedical Co., Seattle, WA) antibodies for 2 h at room temperature, washed and then incubated with biotinylated secondary antibody for 45 min followed by incubation with ABC reagent. After washing in PBS, sections were developed in DAB solution until the desired staining intensity was achieved. Finally, the sections were counterstained with hematoxylin.

Statistical analysis

The data were expressed as the mean \pm standard deviation (SD). Statistical significances of differences among treatment groups were determined by One-way analysis of variance (ANOVA). A p-value of < 0.05 was considered as statistically significant.

Results

C3G inhibits multiple UVB-induced cutaneous edema, hyperplasia and infiltration of leukocytes in SKH-1 hairless mice skin

UVB irradiation leads to cutaneous edema, hyperplasia, erythema, infiltration of leukocytes, dilation of dermal blood vessels and vascular hyperpermeability (Sharma and Katiyar, 2010). In the present study, we assessed the effect of C3G (Fig. 1A) on skin edema in UVB exposed SKH-1 hairless mouse. Bifold-skin thickness an indicator of vascular permeability

and edema was measured 2 h post UVB radiation. Exposure of mouse skin to UVB radiation resulted in a significant increase in bifold-skin thickness compared to control and C3G alone treated animals (Fig. 1B). We next evaluated the effect of C3G on UVB-mediated induction of epidermal hyperplasia and infiltration of leukocytes, 24 h post UVB radiation. Hematoxylin-eosin staining of mouse dorsal skin sections revealed that UVB irradiation to the mouse skin resulted in hyperplasia, and mixed cell infiltration in the dermis (Fig. 1C). As expected, these effects of UVB-induced infiltration of leukocytes and epidermal hyperplasia were inhibited by topical administration of C3G

Considering that multiple exposure of the skin to UVB irradiation induces a pronounced inflammation, the sub-maximal dose of UVB irradiation capable of inducing the increase in the MPO activity was determined. Multiple UVB dose resulted in a 2.0-fold increase in myeloperoxidase activity in the irradiated skin compared with the skin that was not exposed to UVB. When C3G was pretreated along with UVB irradiation, MPO activity was decreased significantly ($p < 0.05$) compared to the UVB alone group (Fig. 1D).

C3G inhibits multiple UVB-induced oxidative stress and DNA damage in SKH-1 hairless mice skin

It is well known that UVB irradiation can generate excessive ROS production and cause oxidative DNA damage, resulting in oxidative stress. At the same time, excessive ROS rapidly initiate peroxidation of the unsaturated fatty acids of phospholipids and protein in the keratinocyte membrane, leading to cell death. However, a great number of studies have suggested the photoprotective effect of topical antioxidants, which might be a successful strategy for reducing UV irradiation-induced oxidative damage of the skin (Hsieh *et al.*, 2005; Sumiyoshi and Kimura, 2009; Lee *et al.*, 2013a). LPO induced by ROS is considered one of the major manifestations of oxidative stress (Khan *et al.*, 2012). In the present study, we assessed the effect of topical administration of C3G on multiple UV exposure to mouse skin by measuring the concentration of the short-chain aldehyde, MDA, which is the by-product of LPO. Our results demonstrated that treatment of C3G effectively inhibited the multiple UVB-mediated increase in the levels of epidermal MDA formation compared with UVB alone group (Fig. 2A).

In the same manner as described above, multiple UVB irradiation dose capable of diminishing the GSH activity was determined. Topical treatment of mice skin with C3G before UVB exposure resulted in inhibition of GSH depletion, maintaining a similar level to non-irradiated control group (Fig. 2B). In addition, UVB unexposed skin treated with C3G presented glutathione levels similar to the unexposed controls. Moreover, UVB causes direct DNA damage by oxidation of nucleotides and produces 8-OHdG (Afaq *et al.*, 2007; Arad *et al.*, 2008). Employing immunofluorescence analysis, we assessed the effect of topical application of C3G on UVB-mediated DNA damage in mouse epidermis. UVB irradiation to SKH-1 hairless mouse skin resulted in increased formation of 8-oxodG when compared to their respective control groups (Fig. 2C). In skin samples obtained 24 h after UVB exposure the numbers of 8-oxodG positive cells were significantly higher when compared to their respective control groups. Topical treatment of C3G on SKH-1 hairless mice skin resulted in marked inhibition of UVB-induced formation of 8-oxodG when compared to their respective

UVB alone groups. Cyclobutane pyrimidine dimers (CPD) represent the major UVB induced DNA damage. Therefore, CPD formation was determined to evaluate the protective effect of C3G. UVB irradiation to SKH-1 hairless mouse skin strongly induced CPD formation, and this effect was markedly suppressed by the topical treatment of C3G (Fig. 2D).

C3G inhibits multiple UVB induced COX-2, iNOS and PGE₂ production in SKH-1 hairless mice skin

Studies have demonstrated that the expression of proinflammatory enzymes such as COX-2 and iNOS are induced by UVB exposure (Afaq *et al.*, 2003b; Sharma and Katiyar, 2010; Lee *et al.*, 2013b). Therefore, we determined the effect of C3G on UVB-induced epidermal COX-2 and iNOS protein expression. Western blot analysis revealed that UVB exposure to SKH-1 hairless mice resulted in a marked increase in epidermal COX-2 and iNOS protein expression compared to control group. However, topical application of C3G significantly reduced the protein expression of COX-2 and iNOS when compared to UVB alone group. Topical application of C3G alone did not produce any change in epidermal COX-2 and iNOS proteins expression when compared to control animals (Fig. 3A). Above result was further confirmed by immunohistochemical analysis of COX-2 (Fig. 3B).

The levels of PGE₂ were also determined in these samples. As shown in Fig. 3C, the levels of PGE₂ in the skin of the UVB-exposed mouse skin were significantly higher ($p < 0.05$) than non-UVB-exposed mouse skin samples. Topical treatment of C3G significantly inhibited ($p < 0.05$) UVB-induced elevation in the levels of PGE₂ in the mouse skin.

C3G inhibits multiple UVB induced TNF- α and IL-6 production in SKH-1 hairless mice skin

TNF- α and IL-6 are known to be proinflammatory cytokines that are linked to inflammatory responses by exposure of UVB radiation to skin. Therefore, we examined the TNF- α and IL-6 production by ELISA, western blot and immunofluorescence analysis. In immunofluorescence analysis, TNF- α labeled cell in skin of the C3G treated group were significantly reduced compared to the control group (Fig. 4A). Also, western blot analysis revealed that protein expression of TNF- α was markedly decreased in the C3G treated group compared to respective control (Fig. 4B). Similarly, the levels of both proinflammatory cytokines, TNF- α (Fig. 4C) and IL-6 (Fig. 4D) on C3G treated group were also significantly ($p < 0.05$) suppressed as compared to control by ELISA.

C3G inhibits multiple UVB induced phosphorylation of MAPK proteins in SKH-1 hairless mice skin

Previous studies have shown that UVB induced oxidative stress implicated in the activation of MAPK, which has been associated to play an important role in the promotion of photocarcinogenesis (Afaq *et al.*, 2003a; Vayalil *et al.*, 2003). Therefore, we assessed the effect of topical administration of C3G on SKH-1 hairless mice skin on multiple UVB-induced activation of MAPK family proteins (ERK1/2, p38, JNK1/2 and MKK4) by Western blot analysis. Our results indicate that multiple UVB exposure to mouse skin resulted in increased phosphorylation of ERK1/2, p38, JNK1/2 and MKK4 proteins of MAPK family. As shown in Fig. 5, Western blot analysis revealed that C3G markedly

reduced UVB-mediated phosphorylation of ERK1/2, p38, JNK1/2 and MKK4 proteins as compared to UVB alone group. Treatment of mice with C3G alone did not induce the phosphorylation of ERK1/2, p38, JNK1/2 and MKK4 proteins of MAPK family. Further, the total amount of ERK1/2, JNK, and p38 proteins remained unchanged in each treatment group.

C3G inhibits multiple UVB induced activation of NF- κ B pathway in SKH-1 hairless mice skin

NF- κ B/p65 is a downstream target of the MAPK signal transduction pathways. Our Western blot analysis indicated that chronic exposure of mice to UVB stimulated the phosphorylation of NF- κ B/p65 as compared to non-UVB-exposed control mice. Topical application of C3G markedly inhibited the UVB induced NF- κ B phosphorylation in a dose-dependent manner (Fig. 6A). Above result was further confirmed by immunofluorescence analysis (Fig. 6B). Moreover, C3G also inhibited the translocation of NF- κ B/p65 to the nucleus compared with non-C3G-treated but UVB-exposed mice (Fig. 6C-D). Previous study showed that exposure of UVB radiation resulted in the degradation of I κ B α protein and subsequent activation and translocation of NF- κ B/p65 to the nucleus (Mantena and Katiyar, 2006). To study the inhibitory effect of C3G on UVB-induced degradation of I κ B α , we determined the cytoplasmic level of I κ B α protein expression. In western blot analysis we found that topical application of C3G inhibited UVB-mediated degradation of I κ B α (Fig. 6E-F).

IKK phosphorylates serine residues in I κ B α and its degradation activates NF- κ B. Chronic UVB exposure also resulted in the activation of IKK α and has been shown to be essential for the degradation of I κ B α . Western blot analysis indicated that the activation level of IKK α was higher in the skin of UVB-irradiated mice; however, topical application of C3G inhibited the activation levels of IKK α in cytosols (Fig. 6E-F). The inhibitory effect of C3G on UVB-induced NF- κ B activation was further confirmed using ELISA for NF- κ B/p65 (Fig. 6G).

C3G inhibits multiple UVB induced increases in the levels of cyclin D1 in SKH-1 hairless mice skin

Chronic UVB exposure affects cell cycle regulators in the skin. Enhanced expression of cell cycle regulatory protein, cyclin-D1 has been implicated in photocarcinogenesis. Immunofluorescence analysis showed that UVB exposure increased the cyclin D1 positive cells compared to non-UVB-exposed mouse skin cells. Topical application of C3G inhibited the cyclin D1 expression to a greater extent in SKH-1 hairless mouse skin (Fig.7A). These data were further confirmed by the analysis of mRNA expression by real-time PCR and protein expression levels by western blot analysis, as shown in Fig. 7B and C.

C3G inhibits multiple UVB induced increases in the levels of PCNA in SKH-1 hairless mice skin

PCNA is a marker of cellular proliferation found throughout the basal layer of normal skin and has a unique role in chromosomal DNA replication. It is abundantly increased in malignant skin diseases. Immunofluorescence analyses revealed that exposure of the skin to UVB radiation enhances the proliferation potential of epidermal keratinocytes as indicated

by the staining pattern of PCNA in the epidermis as compared with non-UVB-irradiated skin. Treatment of the skin with C3G inhibited UVB-induced expression of PCNA in skin (Fig. 8A). Similar results were observed by the analysis of mRNA expression and western blot analysis (Fig. 8B and C).

Discussion

Skin cancer is the most common form of cancer in the United States (Rogers *et al.*, 2010). Each year there are more new cases of skin cancer being diagnosed than the combined incidence of cancers of the breast, prostate, lung and colon (Society, 2012). One among five Americans is estimated to develop skin cancer in the course of lifetime (Robinson, 2005). The major causative agent in skin cancer is UV radiation from sunlight (Sarasin, 1999). Chronic exposure to UV radiations leads to skin cancer (Koh, 1995). Given the increasing morbidity, incidence, and cost, research has been focused on exploring novel chemopreventive agents that inhibit nonmelanoma skin cancer formation and progression (Phillips *et al.*, 2013). Natural products have been used for the treatment of various diseases and are becoming an important research area for drug discovery (Pratheeshkumar *et al.*, 2012). Anthocyanins belong to the family of flavonoids and constitute the largest group of water soluble pigments in nature, responsible for the blue and purple colours of many fruits and vegetables, being consequently widespread in the human diet. Previous studies demonstrated the importance of anthocyanins in the prevention and treatment of chronic inflammatory diseases (Miguel, 2011; Hassimotto *et al.*, 2013). C3G belongs to anthocyanin family, the largest group of pigments present in many edible berries, dark grapes, cabbages, and other pigmented foods (Ding *et al.*, 2006). In this study, we have examined the protective ability of C3G against UVB-induced photodamage.

UVB irradiation clearly induces inflammatory responses, marked by elevated MPO activity (Fazekas *et al.*, 2003) and edema represented by an increase in skin thickness (Ahmad *et al.*, 2001). MPO is an enzyme found primarily in the azurophilic granules of the neutrophils and has been used extensively as a biochemical marker of granulocyte infiltration into various tissues (Jantschko *et al.*, 2005). In our study, chronic UVB exposure significantly increased the MPO enzyme activity (2 fold) and skin thickness compared with the untreated group. Topical application of C3G was able to reduce UVB-induced MPO activity and skin thickness.

Oxidative stress is the result of an imbalance between ROS and the antioxidant defence system. It is well established that UVB radiation exposure to skin results in the depletion of antioxidant defence capabilities at the UV-irradiated site. ROS plays a significant role in UVB-induced skin carcinogenesis (Agar *et al.*, 2004; Halliday, 2005). UV-induced oxidative stress is countered in the body by endogenous antioxidants that neutralize the ROS before they produce oxidative changes in the tissues (Podda and Grundmann-Kollmann, 2001). GSH is considered to be a free radical-scavenger and a cofactor for protective enzymes, which plays a pivotal role in the cellular defence against oxidative damage. UVB irradiation leads to decreased levels of GSH due to leakage and oxidation of GSH (Merwald *et al.*, 2005). In this study, we examined the effect of C3G on antioxidant status in mice skin

under chronic UVB irradiation. The GSH content was significantly reduced after chronic UVB exposure in mice skin. This was markedly inhibited by the topical application of C3G.

The UVB-induced oxidation of lipids is another important indication of oxidative stress. The level of lipid peroxidation has been significantly increased in UVB-exposed mice skin. UVB-induced infiltration and accumulation of activated macrophages and polymorphonuclear neutrophil is a characteristic feature of skin inflammation (Lee *et al.*, 2013b). Electron transfer or singlet molecular oxygen produced by UVB radiation targets DNA base guanine, giving rise to 8-hydroxy-2-deoxyguanosine (8-OHdG) in the DNA strands (Cadet *et al.*, 1999). This is one of the well-known biomarker of oxidative stress and the major mutagenic form of oxidative DNA damage (Barzilai and Yamamoto, 2004). Our results show that C3G renders protection against UVB-radiation-induced oxidation of lipids and oxidative DNA damage in Skh-1 mice skin. Similar results were observed by the topical application of quercitrin on mice skin (Yin *et al.*, 2013).

COX-2 plays a key role in UVB-induced inflammation by catalyzing the generation of PGE₂ from prostanoid precursors (Fischer *et al.*, 2007). Overexpression of COX-2 has been demonstrated in different animal models of inflammation and tumors (Pratheeshkumar and Kuttan, 2010; Pratheeshkumar and Kuttan, 2011a; Son *et al.*, 2013). Therefore, the inhibition of COX-2 expression would be expected to suppress the development of skin cancer. Nitric oxide (NO) has been proposed to be an important mediator of inflammation and overexpressed iNOS has also been detected in several human tumors (Radomski *et al.*, 1991; Gallo *et al.*, 1998; Chiang *et al.*, 2005; Cherng *et al.*, 2011). Previous studies indicate a link between iNOS and COX-2 expression (Yoshida *et al.*, 2006; Cherng *et al.*, 2011). Consistent with this report, our study showed increased COX-2, iNOS, and PGE₂ levels in UVB-exposed mouse skin and topical C3G treatment could effectively suppress them. Along with these proinflammatory mediators, proinflammatory cytokines such as tumor necrosis factor- α (TNF- α) and Interleukine-6 (IL-6) have been shown to be critical cytokines involved in UVB induced inflammation and carcinogenesis (Sharma and Katiyar, 2010). Our data indicated that topical application of C3G significantly inhibited UVB-induced expression of proinflammatory cytokines in mouse skin.

Nuclear factor (NF)- κ B is a ubiquitous nuclear transcription factor responsive to diverse stimuli, such as TNF, UV, interleukins, endotoxins, etc. (Pratheeshkumar and Kuttan, 2011b). Aberrant, sustained activation of NF- κ B has been reported in numerous tumors and was implicated in various stages of photocarcinogenesis (Khan *et al.*, 2012; Wang *et al.*, 2012). NF- κ B is found in an inactive cytoplasmic form, bound to a family of inhibitory proteins termed I κ Bs. Upon activation, I κ B becomes phosphorylated, a process that targets it for ubiquitination and degradation by the proteasome, resulting in the rapid translocation of NF- κ B to the nucleus, where it binds to κ B binding sites in the promoter region of target genes, and induces the transcription of pro-inflammatory mediators, including iNOS, COX-2, TNF- α , IL-6 and others (Perkins, 1997; Wang *et al.*, 2012). In the present study, topical treatment with C3G effectively inhibited the activation and nuclear translocation of NF- κ B/p65 in UVB exposed mice skin. Again C3G also inhibited the UVB induced degradation of I κ B α protein. Collectively, our results clearly demonstrate that topical treatment of C3G prevented the UVB-induced activation and nuclear translocation of NF-

κ B/p65 through the inhibition of activation of IKK α and degradation of I κ B α proteins in mice skin.

MAPK are made up of three family members that include extracellular-signal-related protein kinases (ERKs), c-JUN N-terminal kinases stress-activated protein kinases (JNKs/SAPs) and p38 kinases (Einspahr *et al.*, 2008). During the activation of p38MAPK, several upstream kinases, including MAP kinase kinases (MKK) are also involved. Previous studies have shown that UVB mediated oxidative stress modulates the level of phosphorylated MAPKs including ERK1/2, JNK, and p38, which has been proved to play a role in carcinogenesis (Yoon *et al.*, 2010; Dickinson *et al.*, 2011). Moreover, ERK and p38 proteins of MAPK family have been shown to modulate NF- κ B activation (Sharma and Katiyar, 2010). In the present study, it has been shown that C3G inhibited UVB-induced phosphorylation of ERK, p38 MAPK, JNK and MKK4 on mice skin.

Chronic inflammation is also linked to enhanced cell proliferation which is the hallmark of tumor cells (Gu *et al.*, 2007). The measurement of biomarkers of cellular proliferation, such as epidermal PCNA and cyclin D1 has been used to determine the grade of proliferating potential during tumorigenesis, as well as in predicting the prognosis of malignant tumors (Zhaorigetu *et al.*, 2003; Sharma and Katiyar, 2010). In the present study, topical application of mice with C3G showed a highly significant inhibition of UVB-induced epidermal thickening and decreased mRNA and protein expression of PCNA and cyclin D1. Similar results were observed in UVB-exposed skin by dietary GSPs (Sharma and Katiyar, 2010).

Taken together, these data demonstrate that topical application of C3G provides protection to mouse skin against the adverse effects of UVB radiation by regulating UVB-induced inflammation mediated signalling pathways. This study suggests the potential efficacy of C3G against UVB-induced inflammation related skin disease and skin cancer.

Acknowledgement

This research was supported by National Institutes of Health (R01ES017244, R01ES015518, R01ES020870).

ABBREVIATIONS

COX-2	cyclooxygenase-2
IL	interleukin
MPO	myeloperoxidase
PCNA	proliferating cell nuclear antigen
PGE₂	prostaglandin E2
TNF-α	tumor necrosis factor- α
iNOS	inducible nitric oxide synthase

References

- Afaq F, Adhami VM, Ahmad N. Prevention of short-term ultraviolet B radiation-mediated damages by resveratrol in SKH-1 hairless mice. *Toxicology and applied pharmacology*. 2003a; 186:28–37. [PubMed: 12583990]
- Afaq F, Adhami VM, Ahmad N, Mukhtar H. Inhibition of ultraviolet B-mediated activation of nuclear factor κ B in normal human epidermal keratinocytes by green tea Constituent (–)-epigallocatechin-3-gallate. *Oncogene*. 2003b; 22:1035–1044. [PubMed: 12592390]
- Afaq F, Syed DN, Malik A, Hadi N, Sarfaraz S, Kweon M-H, Khan N, Zaid MA, Mukhtar H. Delphinidin, an anthocyanidin in pigmented fruits and vegetables, protects human HaCaT keratinocytes and mouse skin against UVB-mediated oxidative stress and apoptosis. *Journal of Investigative Dermatology*. 2007; 127:222–232. [PubMed: 16902416]
- Agar NS, Halliday GM, Barnetson RS, Ananthaswamy HN, Wheeler M, Jones AM. The basal layer in human squamous tumors harbors more UVA than UVB fingerprint mutations: a role for UVA in human skin carcinogenesis. *Proceedings of the National Academy of Sciences of the United States of America*. 2004; 101:4954–4959. [PubMed: 15041750]
- Ahmad N, Gilliam AC, Katiyar SK, O'Brien TG, Mukhtar H. A definitive role of ornithine decarboxylase in photocarcinogenesis. *The American journal of pathology*. 2001; 159:885–892. [PubMed: 11549581]
- Ananthaswamy HN, Pierceall WE. Molecular mechanisms of ultraviolet radiation carcinogenesis. *Photochemistry and photobiology*. 1990; 52:1119–1136. [PubMed: 2087500]
- Arad S, Zattra E, Hebert J, Epstein EH Jr, Goukassian DA, Gilchrest BA. Topical Thymidine Dinucleotide Treatment Reduces Development of Ultraviolet-Induced Basal Cell Carcinoma in *i>Pch-1</i> Mice. *The American journal of pathology*. 2008; 172:1248–1255. [PubMed: 18403589]*
- Barzilai A, Yamamoto K-I. DNA damage responses to oxidative stress. *DNA repair*. 2004; 3:1109–1115. [PubMed: 15279799]
- Burns EM, Tober KL, Riggenbach JA, Schick JS, Lamping KN, Kusewitt DF, Young GS, Oberyszyn TM. Preventative topical diclofenac treatment differentially decreases tumor burden in male and female Skh-1 mice in a model of UVB-induced cutaneous squamous cell carcinoma. *Carcinogenesis*. 2013; 34:370–377. [PubMed: 23125227]
- Cadet J, Douki T, Pouget J-P, Ravanat J-L. Singlet oxygen DNA damage products: formation and measurement. *Methods in enzymology*. 1999; 319:143–153. [PubMed: 10907507]
- Chen P-N, Chu S-C, Chiou H-L, Chiang C-L, Yang S-F, Hsieh Y-S. Cyanidin 3-glucoside and peonidin 3-glucoside inhibit tumor cell growth and induce apoptosis in vitro and suppress tumor growth in vivo. *Nutrition and cancer*. 2005; 53:232–243. [PubMed: 16573384]
- Cherng JM, Tsai KD, Perng DS, Wang JS, Wei CC, Lin JC. Diallyl sulfide protects against ultraviolet B-induced skin cancers in SKH-1 hairless mouse: analysis of early molecular events in carcinogenesis. *Photodermatology, photoimmunology & photomedicine*. 2011; 27:138–146.
- Chiang YM, Lo CP, Chen YP, Wang SY, Yang NS, Kuo YH, Shyur LF. Ethyl caffeate suppresses NF- κ B activation and its downstream inflammatory mediators, iNOS, COX-2, and PGE₂ in vitro or in mouse skin. *British journal of pharmacology*. 2005; 146:352–363. [PubMed: 16041399]
- Choi YJ, Uehara Y, Park JY, Kim SJ, Kim SR, Lee HW, Moon HR, Chung HY. MHY884, a newly synthesized tyrosinase inhibitor, suppresses UVB-induced activation of NF- κ B signaling pathway through the downregulation of oxidative stress. *Bioorganic & Medicinal Chemistry Letters*. 2014
- de Gruijl FR. Photocarcinogenesis: UVA vs. UVB radiation. *Skin Pharmacology and Physiology*. 2002; 15:316–320.
- Dickinson SE, Olson ER, Zhang J, Cooper SJ, Melton T, Criswell PJ, Casanova A, Dong Z, Hu C, Saboda K. p38 MAP kinase plays a functional role in UVB-Induced mouse skin carcinogenesis. *Molecular carcinogenesis*. 2011; 50:469–478. [PubMed: 21268131]
- Ding M, Feng R, Wang SY, Bowman L, Lu Y, Qian Y, Castranova V, Jiang B-H, Shi X. Cyanidin-3-glucoside, a natural product derived from blackberry, exhibits chemopreventive and chemotherapeutic activity. *Journal of Biological Chemistry*. 2006; 281:17359–17368. [PubMed: 16618699]

- Ding S-Z, Yang Y-X, Li X-L, Michelli-Rivera A, Han S-Y, Wang L, Pratheeshkumar P, Wang X, Lu J, Yin Y-Q. Epithelial–mesenchymal transition during oncogenic transformation induced by hexavalent chromium involves reactive oxygen species-dependent mechanism in lung epithelial cells. *Toxicology and applied pharmacology*. 2013; 269:61–71. [PubMed: 23518002]
- Einspahr JG, Timothy Bowden G, Alberts DS, McKenzie N, Saboda K, Warneke J, Salasche S, Ranger-Moore J, Curiel-Lewandrowski C, Nagle RB. Cross-validation of Murine UV Signal Transduction Pathways in Human Skin†. *Photochemistry and photobiology*. 2008; 84:463–476. [PubMed: 18248498]
- Fazekas Z, Gao D, Saladi RN, Lu Y, Lebwohl M, Wei H. Protective effects of lycopene against ultraviolet B-induced photodamage. *Nutrition and cancer*. 2003; 47:181–187. [PubMed: 15087271]
- Fischer SM, Pavone A, Mikulec C, Langenbach R, Rundhaug JE. Cyclooxygenase-2 expression is critical for chronic UV-induced murine skin carcinogenesis. *Molecular carcinogenesis*. 2007; 46:363–371. [PubMed: 17219415]
- Gallo O, Fini-Storchi I, Vergari WA, Masini E, Morbidelli L, Ziche M, Franchi A. Role of nitric oxide in angiogenesis and tumor progression in head and neck cancer. *Journal of the National Cancer Institute*. 1998; 90:587–596. [PubMed: 9554441]
- Gu M, Singh RP, Dhanalakshmi S, Agarwal C, Agarwal R. Silibinin inhibits inflammatory and angiogenic attributes in photocarcinogenesis in SKH-1 hairless mice. *Cancer research*. 2007; 67:3483–3491. [PubMed: 17409458]
- Halliday GM. Inflammation, gene mutation and photoimmunosuppression in response to UVR-induced oxidative damage contributes to photocarcinogenesis. *Mutation Research/Fundamental and Molecular Mechanisms of Mutagenesis*. 2005; 571:107–120.
- Hassimotto NMA, Moreira V, Nascimento N.G.d. Souto P.C.M.d.C. Teixeira C, Lajolo FM. Inhibition of carrageenan-induced acute inflammation in mice by oral administration of anthocyanin mixture from wild mulberry and cyanidin-3-glucoside. *BioMed research international*. 20132013
- Hsieh C-L, Yen G-C, Chen H-Y. Antioxidant activities of phenolic acids on ultraviolet radiation-induced erythrocyte and low density lipoprotein oxidation. *Journal of agricultural and food chemistry*. 2005; 53:6151–6155. [PubMed: 16029010]
- Jantschko W, Furtmüller PG, Zederbauer M, Neugschwandtner K, Lehner I, Jakopitsch C, Arnhold J, Obinger C. Exploitation of the unusual thermodynamic properties of human myeloperoxidase in inhibitor design. *Biochemical pharmacology*. 2005; 69:1149–1157. [PubMed: 15794935]
- Khan N, Syed DN, Pal HC, Mukhtar H, Afaq F. Pomegranate Fruit Extract Inhibits UVB-induced Inflammation and Proliferation by Modulating NF- κ B and MAPK Signaling Pathways in Mouse Skin†. *Photochemistry and photobiology*. 2012; 88:1126–1134. [PubMed: 22181855]
- Koh HK. Preventive strategies and research for ultraviolet-associated cancer. *Environmental health perspectives*. 1995; 103:255. [PubMed: 8741794]
- Lee C-W, Ko H-H, Chai C-Y, Chen W-T, Lin C-C, Yen F-L. Effect of *Artocarpus communis* Extract on UVB Irradiation-Induced Oxidative Stress and Inflammation in Hairless Mice. *International journal of molecular sciences*. 2013a; 14:3860–3873. [PubMed: 23403620]
- Lee JA, Jung BG, Kim TH, Lee SG, Park YS, Lee BJ. Dietary Feeding of *Opuntia Humifusa* Inhibits UVB Radiation-Induced Carcinogenesis by Reducing Inflammation and Proliferation in Hairless Mouse Model. *Photochemistry and photobiology*. 2013b; 89:1208–1215. [PubMed: 23789636]
- Mantena SK, Katiyar SK. Grape seed proanthocyanidins inhibit UV-radiation-induced oxidative stress and activation of MAPK and NF- κ B signaling in human epidermal keratinocytes. *Free Radical Biology and Medicine*. 2006; 40:1603–1614. [PubMed: 16632120]
- Merwald H, Klosner G, Kokesch C, Der-Petrossian M, Hönigsmann H, Trautinger F. UVA-induced oxidative damage and cytotoxicity depend on the mode of exposure. *Journal of Photochemistry and Photobiology B: Biology*. 2005; 79:197–207.
- Miguel M. Anthocyanins: Antioxidant and/or anti-inflammatory activities. *J Appl Pharm Sci*. 2011; 1:7–15.
- Perkins ND. Achieving transcriptional specificity with NF- κ B. *The international journal of biochemistry & cell biology*. 1997; 29:1433–1448. [PubMed: 9570137]

- Phillips J, Moore-Medlin T, Sonavane K, Ekshyyan O, McLarty J, Nathan C-AO. Curcumin Inhibits UV Radiation-Induced Skin Cancer in SKH-1 Mice. *Otolaryngology--Head and Neck Surgery*. 2013; 148:797–803. [PubMed: 23386626]
- Podda M, Grundmann-Kollmann M. Low molecular weight antioxidants and their role in skin ageing. *Clinical and experimental dermatology*. 2001; 26:578–582. [PubMed: 11696061]
- Pratheeshkumar P, Kuttan G. *Cardiospermum halicacabum* inhibits cyclophosphamide induced immunosuppression and oxidative stress in mice and also regulates iNOS and COX-2 gene expression in LPS stimulated macrophages. *Asian Pac. J. Cancer Prev*. 2010; 11:1245–1252. [PubMed: 21198271]
- Pratheeshkumar P, Kuttan G. Modulation of immune response by *Vernonia cinerea* L. inhibits the proinflammatory cytokine profile, iNOS, and COX-2 expression in LPS-stimulated macrophages. *Immunopharmacology and immunotoxicology*. 2011a; 33:73–83. [PubMed: 20367552]
- Pratheeshkumar P, Kuttan G. Vernolide-A, a sesquiterpene lactone from *Vernonia cinerea*, induces apoptosis in B16F-10 melanoma cells by modulating p53 and caspase-3 gene expressions and regulating NF- κ B-mediated bcl-2 activation. *Drug and chemical toxicology*. 2011b; 34:261–270. [PubMed: 21649480]
- Pratheeshkumar P, Sreekala C, Zhang Z, Budhraj A, Ding S, Son Y-O, Wang X, Hitron A, Hyun-Jung K, Wang L. Cancer prevention with promising natural products: mechanisms of action and molecular targets. *Anti-Cancer Agents in Medicinal Chemistry (Formerly Current Medicinal Chemistry-Anti-Cancer Agents)*. 2012; 12:1159–1184.
- Radomski MW, Jenkins DC, Holmes L, Moncada S. Human colorectal adenocarcinoma cells: differential nitric oxide synthesis determines their ability to aggregate platelets. *Cancer research*. 1991; 51:6073–6078. [PubMed: 1718593]
- Robinson JK. Sun exposure, sun protection, and vitamin D. *Jama*. 2005; 294:1541–1543. [PubMed: 16193624]
- Rogers HW, Weinstock MA, Harris AR, Hinckley MR, Feldman SR, Fleischer AB, Coldiron BM. Incidence estimate of nonmelanoma skin cancer in the United States, 2006. *Archives of dermatology*. 2010; 146:283–287. [PubMed: 20231499]
- Sano Y, Park JM. Loss of Epidermal p38 α Signaling Prevents Ultraviolet Radiation-Induced Inflammation via Acute and Chronic Mechanisms. *Journal of Investigative Dermatology*. 2014
- Sarasin A. The molecular pathways of ultraviolet-induced carcinogenesis. *Mutation Research/ Fundamental and Molecular Mechanisms of Mutagenesis*. 1999; 428:5–10.
- Sharma SD, Katiyar SK. Dietary grape seed proanthocyanidins inhibit UVB-induced cyclooxygenase-2 expression and other inflammatory mediators in UVB-exposed skin and skin tumors of SKH-1 hairless mice. *Pharmaceutical research*. 2010; 27:1092–1102. [PubMed: 20143255]
- Sharma SD, Meeran SM, Katiyar SK. Dietary grape seed proanthocyanidins inhibit UVB-induced oxidative stress and activation of mitogen-activated protein kinases and nuclear factor- κ B signaling in in vivo SKH-1 hairless mice. *Molecular cancer therapeutics*. 2007; 6:995–1005. [PubMed: 17363493]
- Shih P-H, Yeh C-T, Yen G-C. Effects of anthocyanidin on the inhibition of proliferation and induction of apoptosis in human gastric adenocarcinoma cells. *Food and chemical toxicology*. 2005; 43:1557–1566. [PubMed: 15964118]
- Society AC. *Cancer Facts & Figures 2012*. 2012
- Son Y-O, Pratheeshkumar P, Wang L, Wang X, Fan J, Kim D-H, Lee J-Y, Zhang Z, Lee J-C, Shi X. Reactive oxygen species mediate Cr (VI)-induced carcinogenesis through PI3K/AKT-dependent activation of GSK-3 β / β -catenin signaling. *Toxicology and applied pharmacology*. 2013; 271:239–248. [PubMed: 23707771]
- Sumiyoshi M, Kimura Y. Effects of a turmeric extract (< i> Curcuma longa</i>) on chronic ultraviolet B irradiation-induced skin damage in melanin-possessing hairless mice. *Phytomedicine*. 2009; 16:1137–1143. [PubMed: 19577913]
- Vaid M, Sharma SD, Katiyar SK. Proanthocyanidins Inhibit Photocarcinogenesis through Enhancement of DNA Repair and Xeroderma Pigmentosum Group A-Dependent Mechanism. *Cancer Prevention Research*. 2010; 3:1621–1629. [PubMed: 20947490]

- Vayalil PK, Elmets CA, Katiyar SK. Treatment of green tea polyphenols in hydrophilic cream prevents UVB-induced oxidation of lipids and proteins, depletion of antioxidant enzymes and phosphorylation of MAPK proteins in SKH-1 hairless mouse skin. *Carcinogenesis*. 2003; 24:927–936. [PubMed: 12771038]
- Wang Q-S, Xiang Y, Cui Y-L, Lin K-M, Zhang X-F. Dietary blue pigments derived from genipin, attenuate inflammation by inhibiting LPS-induced iNOS and COX-2 expression via the NF- κ B inactivation. *PLoS one*. 2012; 7:e34122. [PubMed: 22479539]
- Xu M, Bower KA, Wang S, Frank JA, Chen G, Ding M, Wang S, Shi X, Ke Z, Luo J. Cyanidin-3-glucoside inhibits ethanol-induced invasion of breast cancer cells overexpressing ErbB2. *Molecular cancer*. 2010; 9:285. [PubMed: 21034468]
- Yin Y, Li W, Son Y-O, Sun L, Lu J, Kim D, Wang X, Yao H, Wang L, Pratheeshkumar P. Quercitrin protects skin from UVB-induced oxidative damage. *Toxicology and applied pharmacology*. 2013; 269:89–99. [PubMed: 23545178]
- Yoon JH, Lim T-G, Lee KM, Jeon AJ, Kim SY, Lee KW. Tangeretin reduces ultraviolet B (UVB)-induced cyclooxygenase-2 expression in mouse epidermal cells by blocking mitogen-activated protein kinase (MAPK) activation and reactive oxygen species (ROS) generation. *Journal of agricultural and food chemistry*. 2010; 59:222–228. [PubMed: 21126077]
- Yoshida E, Watanabe T, Takata J, Yamazaki A, Karube Y, Kobayashi S. Topical application of a novel, hydrophilic γ -tocopherol derivative reduces photo-inflammation in mice skin. *Journal of Investigative Dermatology*. 2006; 126:1633–1640. [PubMed: 16543897]
- Zhaorigetu S, Yanaka N, Sasaki M, Watanabe H, Kato N. Inhibitory effects of silk protein, sericin on UVB-induced acute damage and tumor promotion by reducing oxidative stress in the skin of hairless mouse. *Journal of Photochemistry and Photobiology B: Biology*. 2003; 71:11–17.
- Zheng W, Wang SY. Oxygen radical absorbing capacity of phenolics in blueberries, cranberries, chokeberries, and lingonberries. *Journal of Agricultural and Food Chemistry*. 2003; 51:502–509. [PubMed: 12517117]

Highlights

- C3G inhibited UVB-induced oxidative damage and inflammation.
- C3G inhibited UVB-induced COX-2, iNOS and PGE₂ production.
- C3G inhibited UVB-induced elevated proinflammatory cytokines level.
- C3G inhibited UVB-induced p38 MAP kinase signaling.
- C3G inhibited UVB-induced NF- κ B activation.

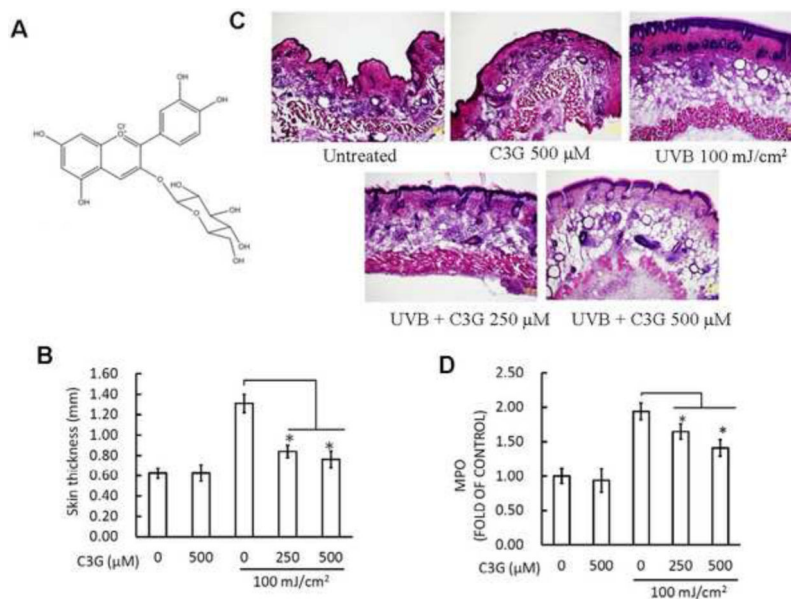


Figure 1.

C3G inhibits UVB induced skin edema. (A) Chemical structure of C3G with a molecular weight of 484.8 g/mol. (B) C3G inhibits UVB-induced hyperplastic response in terms of epidermis thickness (mm). Female SKH-1 mice (6–8weeks, n=8) were UVB irradiated (100 mJ/cm²) three times a week for a total of 10 weeks. The animals were treated topically with either acetone (control group) or C3G (250 and 500 μM in acetone) one day prior to UVB exposure. The Mice were sacrificed after 10 weeks of UVB irradiation; Skin was collected and measured the thickness. Significant difference compared to UVB alone; *p<0.05. (C) Representative micrographs of H&E staining of skin. (D) MPO was determined as a marker of UVB-induced cutaneous infiltration. The levels of UVB-induced MPO were lower in C3G -treated mouse skin than non-C3G-treated UVB irradiated mouse skin. Data are reported as fold change (n=8). Significant difference compared to UVB alone; *p<0.05.

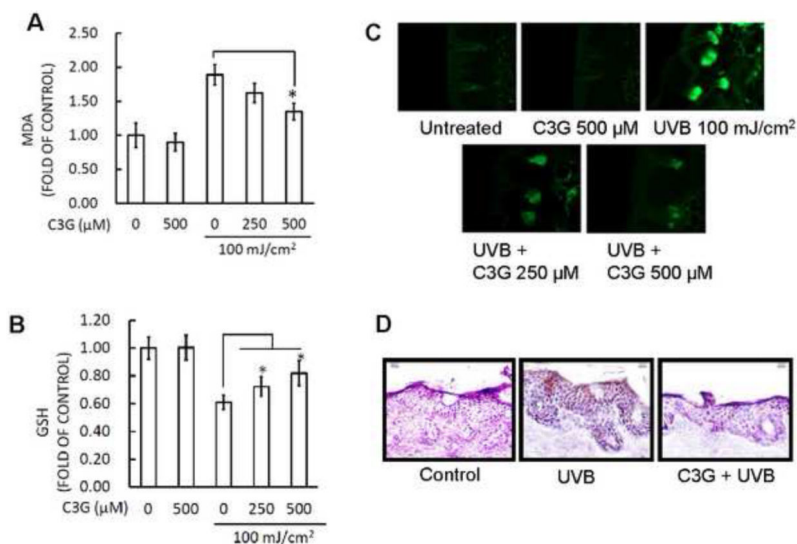


Figure 2.

C3G inhibits UVB induced oxidative stress and DNA damage in mice skin. C3G treatment and UVB irradiation is as described in Fig.1. The animals were sacrificed at the indicated times. Skin samples were collected and homogenized by sonication in ice cold PBS. Tissue lysate was used for the determination of oxidative stress in terms of (A) lipid peroxidation and (B) glutathione depletion (C) C3G inhibited UVB-mediated oxidative DNA damage was detected by immunofluorescence staining of skin cryosections with 8-OHdG antibody and (D) immunoperoxidase staining to detect UVB-induced thymine dimer formation that is dark brown. A representative picture from three independent experiments with similar results is shown.

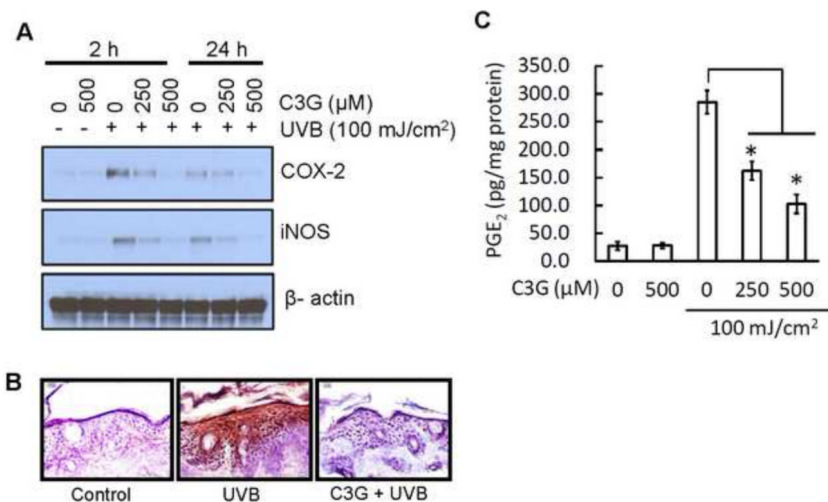
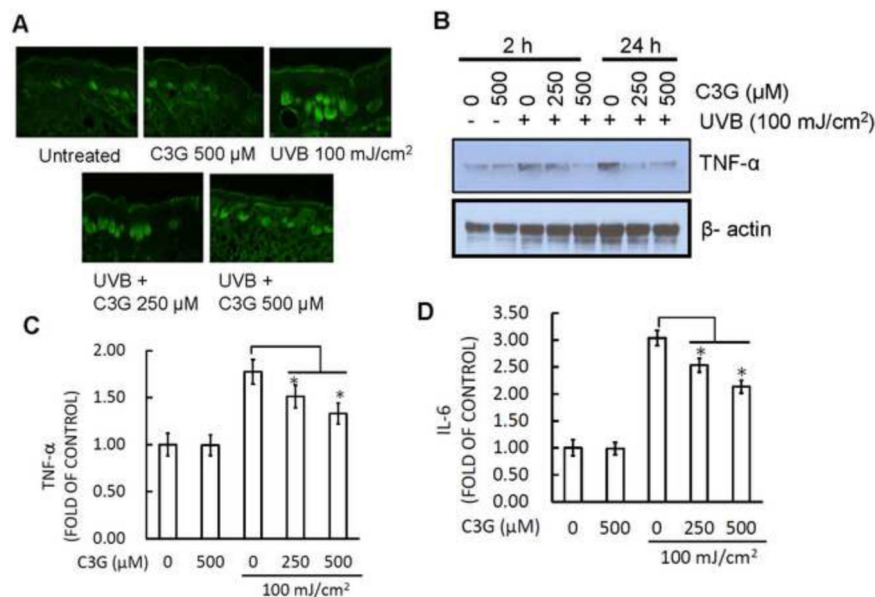


Figure 3. C3G inhibits the expression of COX-2, iNOS and PGE₂ in UVB-irradiated mouse skin. C3G treatment and UVB irradiation is as described in Fig.1. The animals were sacrificed at the indicated times. Tissue lysates were prepared as described in Materials and methods. (A) The protein expressions of COX-2 and iNOS were determined in tissue lysate samples using western blot analysis. Equal loading of protein samples was confirmed using β-actin. (B) Frozen skin sections (5 μM thick) were subjected to immunoperoxidase staining to detect COX-2 expression that is dark brown. (C) Epidermal PGE₂ was determined as a marker of inflammation using Cayman PGE₂ Enzyme immunoassay kit as described in Materials and methods, and the concentration of PGE₂ is expressed in terms of pg per mg protein as a mean ± SD, n=8. Significant difference compared to UVB alone, *p<0.05.

**Figure 4.**

C3G inhibits UVB induced proinflammatory cytokines in mice skin. Mice were treated as described in Fig. 1. (A) The mice were sacrificed after 10 weeks of UVB irradiation and skin samples were subjected to immunofluorescence staining to detect the expression of TNF- α -positive cells following the procedure as described in Materials and Methods. (B) Western blot was employed to determine the TNF- α protein expression. (C-D) The levels of proinflammatory cytokines (TNF- α and IL-6) in tissue samples were determined using cytokine-specific ELISA following the manufacturer's protocol. Significant difference compared to UVB alone, * $p < 0.05$.

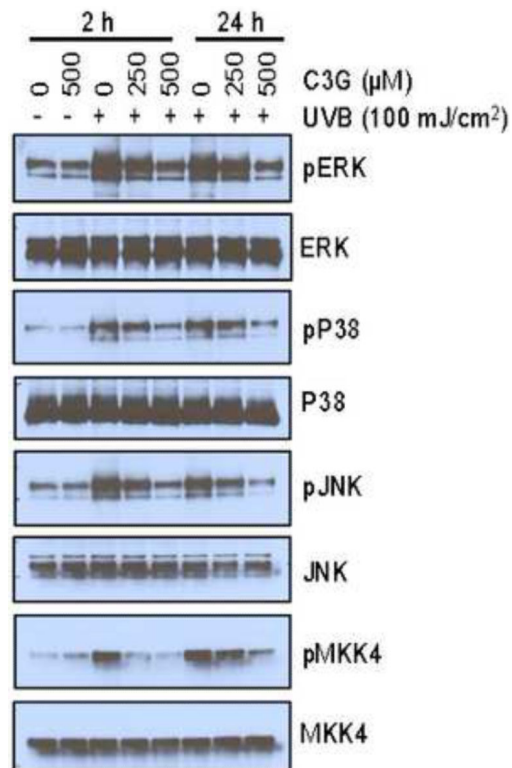


Figure 5.

C3G inhibits UVB induced MAPK signaling in mice skin. Mice were treated as described in Fig. 1. The animals were sacrificed at 2 h and 24 h after 10 weeks of UVB irradiation and tissue lysates were prepared to determine the phosphorylated and total protein levels of ERK1/2, p38, JNK and MKK4 using Western blot analysis, as described under Materials and methods. A representative blot from three independent experiments with identical an observation is shown, and equivalent protein loading was confirmed by probing stripped blots for β -actin as shown.

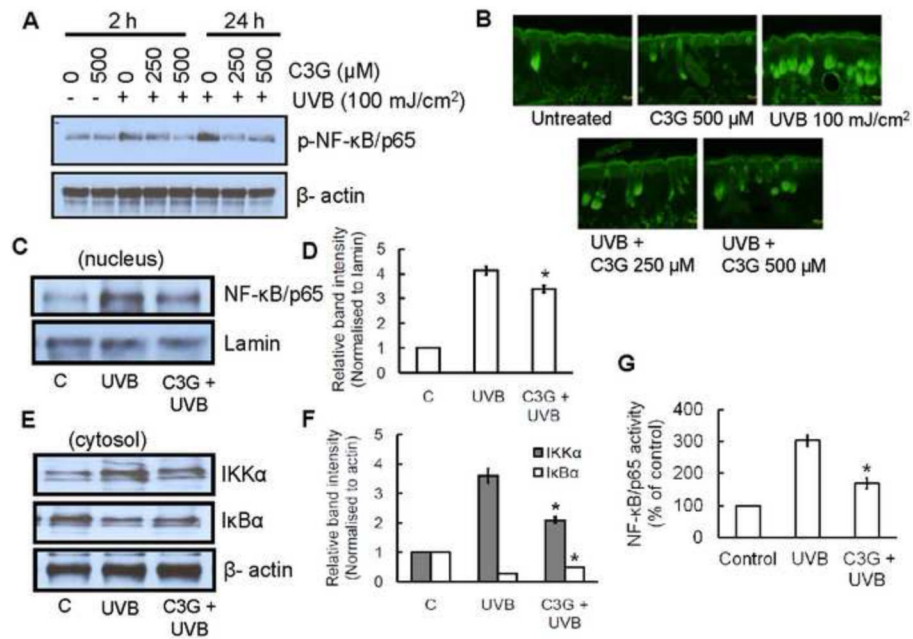


Figure 6.

C3G inhibits UVB induced activation of NF- κ B/p65 and IKK α , and degradation of I κ B α in mice skin. Mice were treated as described in Fig. 1. (A) The phosphorylation/activation of NF- κ B/p65 (B) Immunofluorescence staining of NF- κ B/p65 (C-D) nuclear translocation of NF- κ B/p65 (E-F) activation of IKK α , or degradation of I κ B α in the cytosol was determined by Western blot analysis. The relative intensities of each band after normalization for the levels of laminin/ β -actin are shown under each blot. A representative blot from three independent experiments with identical observations is shown, and equivalent protein loading was confirmed by probing stripped blots for β -actin as shown. (G) The activity of NF- κ B in nuclear fraction of skin lysates was measured using ELISA following the manufacturer's protocol. Significant difference compared to UVB alone, * $p < 0.05$.

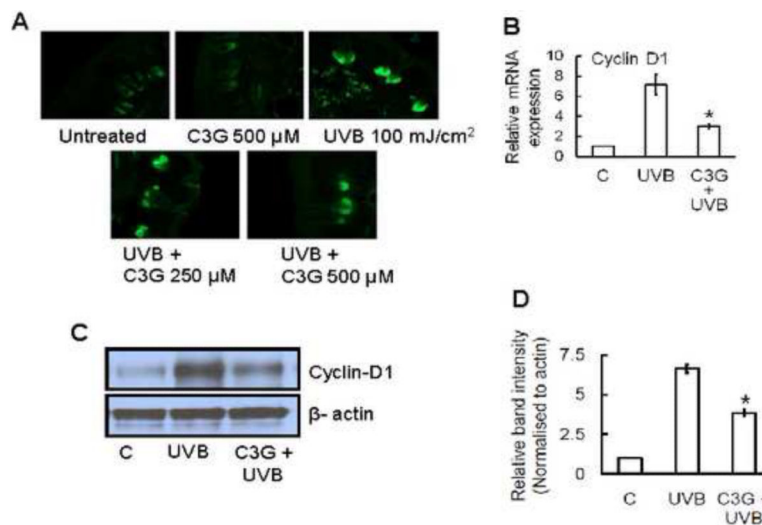


Figure 7. C3G inhibits UVB induced cell proliferation marker, cyclin-D1 in mice skin. Mice were treated as described in Fig. 1. (A) Immunofluorescence detection of cyclin-D1 expression in chronically UVB-exposed mouse skin. The analysis of epidermal cyclin-D1 expressions was performed using (B) real time PCR and (C-D) Western blotting, as described in Materials and methods. The relative intensities of each band after normalization for the levels of β -actin are shown under each blot. Significant difference compared to UVB alone, * $p < 0.05$.

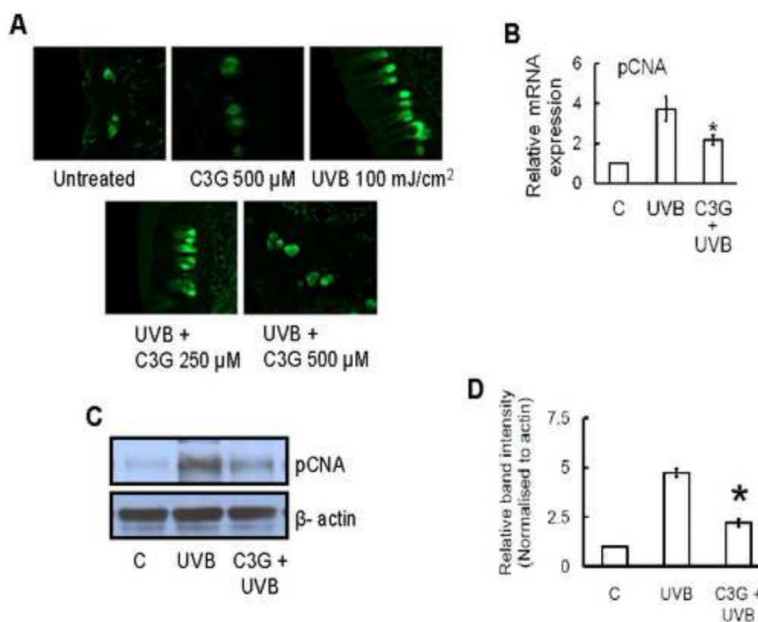


Figure 8.

C3G inhibits UVB induced cell proliferation marker, pCNA in mice skin. Mice were treated as described in Fig. 1. (A) Immunofluorescence detection of pCNA expression in chronically UVB-exposed mouse skin. The analysis of epidermal pCNA expressions was performed using (B) real time PCR and (C-D) Western blotting, as described in Materials and methods. The relative intensities of each band after normalization for the levels of β -actin are shown under each blot. Significant difference compared to UVB alone, * $p < 0.05$.